

FADING OF THE TRANSIENT ANOMALOUS X-RAY PULSAR XTE J1810–197

J. P. HALPERN AND E. V. GOTTHELF

Columbia Astrophysics Laboratory, Columbia University, 550 West 120th Street,
New York, NY 10027-6601; jules@astro.columbia.edu

Received 2004 April 30; accepted 2004 September 22

ABSTRACT

Three observations of the 5.54 s Transient Anomalous X-ray Pulsar XTE J1810–197 obtained over 6 months with the *Newton X-Ray Multi-Mirror Mission (XMM-Newton)* are used to study its spectrum and pulsed light curve as the source fades from outburst. The decay is consistent with an exponential of time constant ≈ 300 days, but not a power law as predicted in some models of sudden deep crustal heating events. All spectra are well fitted by a blackbody plus a steep power law, a problematic model that is commonly fitted to anomalous X-ray pulsars (AXPs). A two-temperature blackbody fit is also acceptable, and better motivated physically in view of the faint optical/IR fluxes, the X-ray pulse shapes that weakly depend on energy in XTE J1810–197, and the inferred emitting areas that are less than or equal to the surface area of a neutron star. The fitted temperatures remained the same while the flux declined by 46%, which can be interpreted as a decrease in area of the emitting regions. The pulsar continues to spin down, albeit at a reduced rate of $(5.1 \pm 1.6) \times 10^{-12} \text{ s s}^{-1}$. The inferred characteristic age $\tau_c \equiv P/2\dot{P} \approx 17,000$ yr, magnetic field strength $B_s \approx 1.7 \times 10^{14}$ G, and outburst properties are consistent with both the outburst and quiescent X-ray luminosities being powered by magnetic field decay, i.e., XTE J1810–197 is a magnetar.

Subject headings: pulsars: general — stars: individual (XTE J1810–197) — stars: neutron — X-rays: stars

1. INTRODUCTION

The bright 5.54 s X-ray pulsar XTE J1810–197 was discovered serendipitously by Ibrahim et al. (2004) using the *Rossi X-ray Timing Explorer (RXTE)*, and was localized in two target-of-opportunity (TOO) observations with the *Chandra X-ray Observatory*, reported by Gotthelf et al. (2004, hereafter Paper I) and Israel et al. (2004). The source had become active sometime between 2002 November 17 and 2003 January 23. The maximum (2–10 keV) flux observed by *RXTE* was $\approx 6 \times 10^{-11}$ ergs $\text{cm}^{-2} \text{ s}^{-1}$, when it was already declining with an exponential time constant of 269 ± 25 days (Ibrahim et al. 2004). Of unique value are all of the archival *Einstein*, *ROSAT*, and *ASCA* detections at the location of XTE J1810–197, which indicate a long-lived quiescent baseline flux of $F_x(0.5 - 10 \text{ keV}) \approx 7 \times 10^{-13}$ ergs $\text{cm}^{-2} \text{ s}^{-1}$ for at least 13 years and possibly for 23 years prior to the onset of the active state (Paper I and Figure 1). Timing of the highly modulated signal over the first 9 months of the outburst indicated rapid spin-down with characteristic age $\tau_c \equiv P/2\dot{P} \leq 7600$ yr, surface magnetic field $B_s \approx 2.6 \times 10^{14}$ G, and spin-down power $\dot{E} \approx 4 \times 10^{33}$ erg s^{-1} (Ibrahim et al. 2004). Deep IR observations (Israel et al. 2004) detected a faint candidate of $K_s = 20.8$, similar to ones associated with other AXPs, within the final 0''6 radius *Chandra* error circle of XTE J1810–197. Variability of the IR source confirmed its identification with XTE J1810–197 (Rea et al. 2004a,b).

The magnetar model (Duncan & Thompson 1992) seems poised to address observational properties of several categories of single, young neutron stars (NSs) that are not powered by rotation. These include the AXPs, Soft Gamma-ray Repeaters (SGRs), and Central Com-

pact Objects (CCOs) within supernova remnants that lack detected periods but whose spectra resemble those of AXPs and SGRs. Such unification is supported by the discovery of transient behavior in AXP-like objects. The first suggested TAXP was AX J1844.8–0256 (Gotthelf & Vasisht 1998). The timing and spectral properties of that 7-s X-ray pulsar are consistent with an AXP, while its flux was found to change by orders-of-magnitude from an “active” pulsar state to a faint “quiescent” state since its discovery. However, the lack of a \dot{P} measurement for AX J1844.8–0256, which was observed serendipitously only once, has left its status as an AXP unconfirmed. With the discovery of the *bona fide* TAXP XTE J1810–197, consideration of possible related observations such as the cooling trend in the post-burst fluxes of SGR 1627–41 (Kouveliotou et al. 2003), SGR 1900+14 (Lenters et al. 2003), and AXP 1E 2259+586 (Woods et al. 2004), and the variable CCO in the young SNR RCW 103 (Gotthelf, Petre, & Hwang 1997; Gotthelf, Petre, & Vasisht 1999a), motivates development of a unified magnetar model for the entire AXP/SGR/CCO family.

Although TAXPs are relatively rare, their short active duty cycle suggests the existence of a significant number of as-yet unrecognized, although not necessarily undetected, young NSs. XTE J1810–197 provides a new window into this population, with a well documented quiescent history and detailed observations during its active, pulsed phase. Monitoring of the fading of XTE J1810–197 takes advantage of a possibly unique opportunity to study evolving spectral and timing behavior of a TAXP, which reveals the time-dependence of the thermal and non-thermal emission mechanisms to which magnetars convert their energy. In particular, the physi-

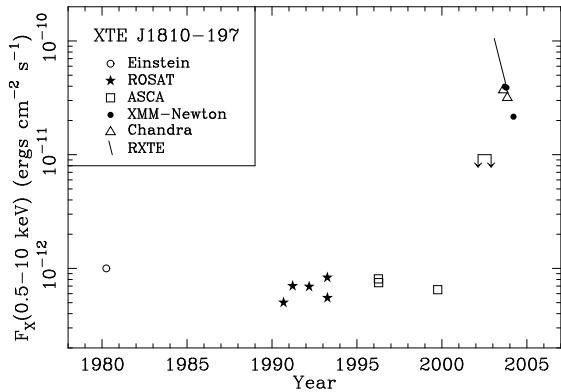


FIG. 1.— The 0.5 – 10 keV flux history of XTE J1810–197 spanning 24 years. The historical data points are from Paper I. The *solid line* is an exponential fit with time constant 269 days to the *RXTE* monitoring from Ibrahim et al. (2004). Upper limits indicated in 2002 are also from several months of monitoring by *RXTE*, which constrains the onset of the outburst to < 2 months before its initial detection in 2003 January.

cal interpretation of the two-component X-ray spectrum that seems characteristic of most AXPs can be investigated in more ways than is possible for a quiescent source. We are beginning such a study with the *XMM-Newton* observations of XTE J1810–197 listed in Table 1.

2. *XMM-Newton* OBSERVATIONS AND RESULTS

The first *XMM-Newton* Target of Opportunity (TOO) observation of XTE J1810–197 was obtained on 2003 September 8 and described in Paper I. A second *XMM-Newton* TOO observation of XTE J1810–197 was performed on 2004 March 11. We use the data obtained with the European Photon Imaging Camera (EPIC, Turner et al. 2003). EPIC consists of three CCD cameras, the EPIC pn and the two EPIC MOS imagers, which are sensitive to X-rays in 0.1 – 10 keV nominal range. The observing modes were different for the two observations. In 2003 September, one of the EPIC MOS cameras was operated “small window” mode, for which the field of view (FOV) of the central CCD was reduced to $1'8 \times 1'8$ and read out in a time of 0.3 s. The second EPIC MOS camera was operated in “full frame” mode, which is read out in 2.7 s integrations over the $30'$ FOV. The EPIC pn was operated in “small window” mode, which provides 6 ms time resolution over a $4'3 \times 4'3$ FOV. In 2004 March, both of the EPIC MOS cameras were operated in “small window” mode, while the EPIC pn was operated in “large window” mode, which provides 48 ms time resolution over a $13'5 \times 26'$ FOV. Thus, all data sets except the “full frame” MOS in 2003 September were of high enough time resolution to study the pulse profiles of XTE J1810–197. In addition, XTE J1810–197 was detected serendipitously in a short observation, as yet unpublished, from the *XMM-Newton* Galactic Plane Survey (Hands et al. 2004) on 2003 October 12. We include results from this survey observation for completeness, including timing information from the pn camera in “full frame” mode with 73.4 ms time resolution.

In order to make the cleanest possible comparison among the *XMM-Newton* observations, we extracted all calibrated photon event data files using the latest version of the *XMM-Newton* Science Analysis System [re-

lease version SAS 6.0.0 (20040309_1146)], by applying the processing chains to each set of Observation Data Files (ODF). Screened photon event lists were generated by applying the standard *XMM-Newton* good-time filter criteria and selecting CCD PATTERN ≤ 4 for our EPIC pn spectral analysis. A total of 11.5 ks, 6.9 ks, and 17.0 ks of good EPIC pn exposure time were acquired during the three observing epochs, which translates to an effective live time of 8.1 ks, 6.2 ks, and 15.8 ks. Resulting background subtracted count rates were 10.6 s^{-1} , 4.8 s^{-1} , and 5.8 s^{-1} , where the second one is affected by vignetting at the off-axis angle of $8'8$. The observations were mostly uncontaminated by flare events. Photon arrival times were converted to the solar system barycenter using the *Chandra* derived coordinates of the source given in Paper I, (J2000) $18^{\text{h}}09^{\text{m}}51.^{\text{s}}08$, $-19^{\circ}43'51''.7$. We manually corrected a jump of +1 s in the EPIC pn photon arrival times that affected part of the 2004 March observation. Timing anomalies are frequent in the pn data; evidently, they have not been completely eliminated in SAS 6.0.0.

2.1. Spectral Modeling

In Table 2, we summarize the results of spectral analysis of previous and new observations. Although of relatively poor quality, the quiescent *ROSAT* spectrum of XTE J1810–197 can be reasonably well fitted with a blackbody of $kT = 0.18 \pm 0.02$ keV covering $1.2 \times 10^{13} \text{ cm}^2$, or 2/3 the area of a 12 km radius NS at $d = 5$ kpc. In contrast, the X-ray spectra in outburst, obtained from the *XMM-Newton* TOO observations, required two components, which is typical of AXPs (e.g., Marsden & White 2001). We fitted *XMM-Newton* data from the EPIC pn CCD only. The fast read out of this instrument ensures that its spectrum is not affected by photon pile-up. Source spectra were accumulated in a $45''$ radius aperture which encloses $\geq 95\%$ of the encircled energy. Background was taken from a circle of the same size displaced 2/3 along the readout direction. The spectra were grouped into bins containing a minimum of 400 counts (including background) and fitted using the XSPEC package. The “wabs” photoelectric absorption cross sections of Morrison & McCammon (1983), not including Thomson scattering, were used with the Anders & Ebihara (1982) abundances. For each model, the column density was treated as a single parameter in a linked fit to all three epochs, after verifying that independent fits yielded consistent values of N_{H} . The other fitted parameters are also consistent with their values obtained in fits with independent N_{H} .

The *XMM-Newton* spectra are equally well fitted by a power-law plus blackbody model, as commonly quoted for AXPs, or by a two-temperature blackbody model that we will argue is more physically motivated. Sample fits are shown in Figure 2. But the ambiguity about which X-ray spectral model is appropriate affects our estimate of the distance to the source by contributing systematic uncertainty to the fitted column density. The X-ray measured $N_{\text{H}} = (1.02 \pm 0.05) \times 10^{22} \text{ cm}^{-2}$ in the case of the power-law plus blackbody model is significantly different from the value of $(0.65 \pm 0.04) \times 10^{22} \text{ cm}^{-2}$ in the double blackbody model (see Table 2). We argued in Paper I that, in either case, XTE J1810–197 is likely to be closer than the neighboring supernova remnant G11.2–0.3, which has an H I absorption kinematic distance of

TABLE 1
XMM-Newton OBSERVATIONS OF XTE J1810–197

Parameter	EPIC pn 2003 Sep 8	EPIC pn 2003 Oct 12	EPIC pn 2004 Mar 11
Off-axis angle (arcmin)	0.0	8.8	0.0
Exposure time (ks)	11.5	6.9	17.0
Live Time (ks)	8.1	6.2	15.8
Count Rate (s^{-1}) ^a	10.6	4.8	5.8
Epoch (MJD/TDB) ^b	52890.5642044	52924.0000320	53075.4999960
Period (s) ^c	5.539344(19) ^c	5.53943(8)	5.539425(16) ^c

^aBackground subtracted EPIC pn count rate corrected for detector dead-time.

^bEpoch of phase zero in Figure 4.

^cIncludes EPIC MOS data. 95% confidence uncertainty in parentheses.

TABLE 2
 SPECTRAL FITS AND FLUXES

Model Parameter	<i>ROSAT</i> /PSPC 1992 Mar 7	2003 Sep 8	<i>XMM-Newton</i> /EPIC pn 2003 Oct 12	2004 Mar 11
Blackbody				
N_H (10^{22} cm $^{-2}$)	0.63 (fixed)
kT_{BB} (keV)	0.18 ± 0.02
BB Area (cm 2)	1.2×10^{13}
Flux (ergs cm $^{-2}$ s $^{-1}$) ^a	6.9×10^{-13}
L_{BB} (bol) (ergs s $^{-1}$)	1.3×10^{34}
χ^2_{ν} (dof)	1.1(13)
Power-law + Blackbody				
N_H (10^{22} cm $^{-2}$) ^b	...	1.02 ± 0.05	1.02 ± 0.05	1.02 ± 0.05
Γ	...	3.87 ± 0.25	3.51 ± 0.15	3.75 ± 0.20
kT_{BB} (keV)	...	0.67 ± 0.01	0.68 ± 0.01	0.68 ± 0.01
BB Area (cm 2)	...	6.2×10^{11}	5.2×10^{11}	2.7×10^{11}
PL Flux (ergs cm $^{-2}$ s $^{-1}$) ^a	...	1.17×10^{-11}	1.42×10^{-11}	8.47×10^{-12}
L_{PL} (ergs s $^{-1}$) ^c	...	2.7×10^{35}	3.6×10^{35}	1.8×10^{35}
BB Flux (ergs cm $^{-2}$ s $^{-1}$) ^a	...	2.80×10^{-11}	2.47×10^{-11}	1.31×10^{-11}
L_{BB} (bol) (ergs s $^{-1}$)	...	1.3×10^{35}	1.1×10^{35}	6.0×10^{34}
Total Flux (ergs cm $^{-2}$ s $^{-1}$) ^a	...	3.97×10^{-11}	3.89×10^{-11}	2.16×10^{-11}
χ^2_{ν} (dof) ^b	...	1.077(187)	1.077(84)	1.077(194)
Double Blackbody				
N_H (10^{22} cm $^{-2}$) ^b	...	0.65 ± 0.04	0.65 ± 0.04	0.65 ± 0.04
kT_1 (keV)	...	0.26 ± 0.02	0.29 ± 0.04	0.27 ± 0.02
kT_2 (keV)	...	0.68 ± 0.02	0.71 ± 0.03	0.70 ± 0.01
BB1 Area (cm 2)	...	1.1×10^{13}	6.6×10^{12}	6.8×10^{12}
BB2 Area (cm 2)	...	6.4×10^{11}	5.1×10^{11}	2.9×10^{11}
BB1 Flux (ergs cm $^{-2}$ s $^{-1}$) ^a	...	4.24×10^{-12}	5.37×10^{-12}	3.52×10^{-12}
BB2 Flux (ergs cm $^{-2}$ s $^{-1}$) ^a	...	3.51×10^{-11}	3.03×10^{-11}	1.78×10^{-11}
L_{BB1} (bol) (ergs s $^{-1}$)	...	5.2×10^{34}	5.1×10^{34}	3.9×10^{34}
L_{BB2} (bol) (ergs s $^{-1}$)	...	1.4×10^{35}	1.3×10^{35}	7.2×10^{34}
Total Flux (ergs cm $^{-2}$ s $^{-1}$) ^a	...	3.93×10^{-11}	3.84×10^{-11}	2.13×10^{-11}
χ^2_{ν} (dof) ^b	...	1.076(187)	1.076(84)	1.076(194)

NOTE. — Uncertainties are 90% confidence for two interesting parameters.

^aAbsorbed flux in the 0.5–10 keV band.

^bParameter derived from a linked fit to all epochs.

^cUnabsorbed luminosity in the 0.5–10 keV band assuming $d = 5$ kpc.

5 kpc (Green et al. 1988) and an X-ray measured column density of $\approx 1.4 \times 10^{22}$ cm $^{-2}$ (Vasisht et al. 1996). With the distance somewhat uncertain, we parameterize derived quantities in terms of d_5 , an upper limit on the distance, in units of 5 kpc.

Considering first the 2003 September observation, the best fit to the power-law plus blackbody model has photon index $\Gamma = 3.87 \pm 0.25$ and $kT_{BB} = 0.67 \pm 0.01$ keV, with a fit statistic of $\chi^2_{\nu} = 1.077$ for 187 degrees of free-

dom. The flux for each of these components is given in Table 2. The blackbody flux is equivalent to a spherical area of $6.2 \times 10^{11} d_5^2$ cm 2 , or $\approx 3\%$ of the surface area of a NS. It is noteworthy that the 2004 March spectrum had nearly identical parameters, with $\Gamma = 3.75 \pm 0.20$ and $kT_{BB} = 0.68 \pm 0.01$ keV, while the fluxes of the power law and blackbody declined by 28% and 53%, respectively.

A two-temperature blackbody model yielded a fit of essentially the same quality, with a fit statistic of

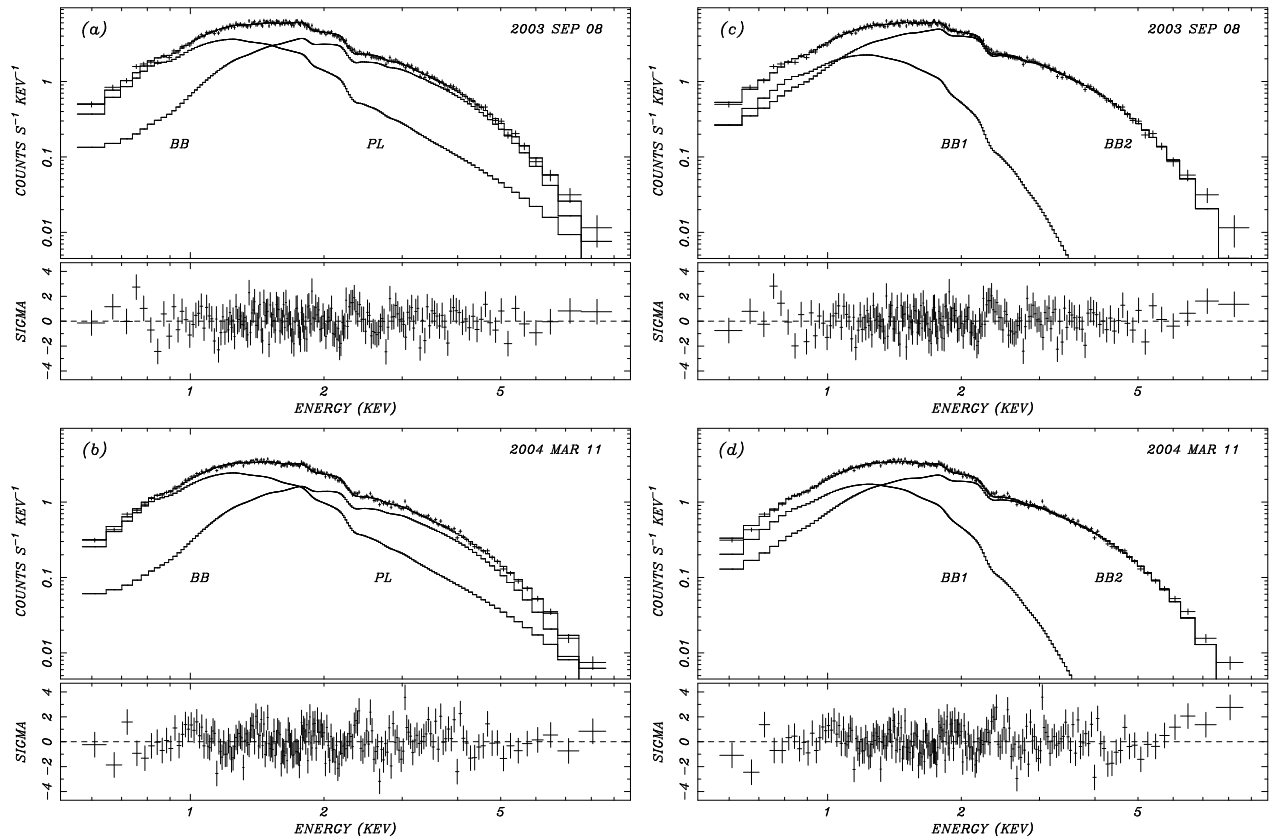


FIG. 2.— *XMM-Newton* EPIC pn spectra of XTE J1810–197 from the earliest and latest epochs, fitted with a power-law plus blackbody model or a double blackbody model as described in the text and in Table 2. Also shown are the residuals from the best-fit models. (a) Power-law plus blackbody fit in 2003 September. (b) Double blackbody fit in 2003 September. (c) Power-law plus blackbody fit in 2004 March. (d) Double blackbody fit in 2004 March.

$\chi^2_{\nu} = 1.076$ for 187 degrees of freedom. The 2003 September spectrum has $kT_1 = 0.26 \pm 0.02$ keV and $kT_2 = 0.68 \pm 0.02$ keV associated with blackbody areas of $1.1 \times 10^{13} d_5^2$ cm² and $6.4 \times 10^{11} d_5^2$ cm² for the cooler and hotter temperatures, respectively, which are $\approx 60\%$ and $\approx 4\%$ of the NS surface. Thus, the power-law component of the previous model is replaced with a cooler blackbody, while the hotter thermal component retains the same parameters in both models. In the double blackbody model, the cooler component covers a large fraction of the NS surface, but at a temperature significantly higher than the quiescent *ROSAT* measured value. In this parameterization, the cooler and hotter blackbody luminosities declined by 25% and 50%, respectively, between 2003 September and 2004 March. Since their temperatures remained the same to within 3% ($kT_1 = 0.27 \pm 0.02$ keV and $kT_2 = 0.70 \pm 0.01$ keV in 2004 March), their decline in luminosity is attributable to a decrease in area.

In order to extract further information about the distribution of emission over the stellar surface, we analyzed phase-resolved spectra by fitting the two-temperature blackbody model to the 2003 September data in 10 phase bins. In particular, we kept the temperatures and column density fixed at the values listed in Table 2 while fitting for the normalization (intensity) in each phase bin. This is equivalent to determining the relative projected area

of emission as a function of rotation phase. This procedure yields acceptable fits in all phase bins, with reduced χ^2 values ranging from 0.73 to 1.21. In nine out of 10 bins, the reduced χ^2 is less than 1.08. Since these fits are statistically acceptable as a set, no significant test can be made for variations in additional parameters such as the temperatures or column density.

The results of the phase-resolved spectral fitting are shown in Figure 3. As can be expected, the intensity of the hot component varies by a large factor, ≈ 3.5 , while the larger cool component varies by only a factor of 1.7. Both components peak at the same phase. This is consistent with the energy-dependent light curves (Fig. 4), in which the pulsed fraction increases with increasing energy. The relative amplitudes and phases of the two components are therefore consistent with the picture of a small, hot region surrounded by a cooler, concentric annulus that occupies of order half the surface area of the star. Neither component goes to zero at any rotation phase. In particular, if the hot component were completely eclipsed, the spectral decomposition in Figure 2 indicates that the light curves at $E > 3$ keV should go to zero, which clearly they do not.

While the overall fits of the two models are of equal quality, the double blackbody model does leave significant residuals above 6 keV, which may be indicative

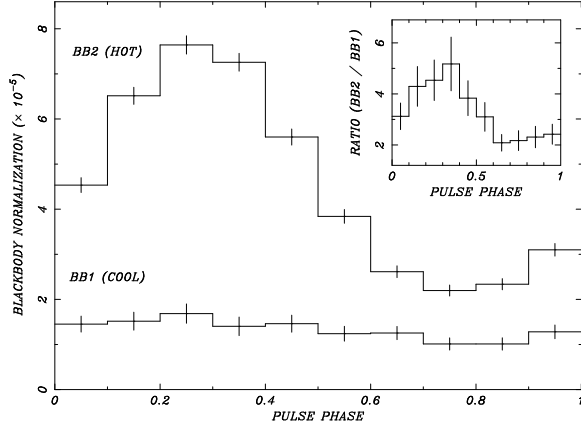


FIG. 3.— Comparison of the two-component blackbody intensities as a function of rotation phase in the 2003 September *XMM-Newton* EPIC pn spectrum. The temperatures kT_1 and kT_2 are held fixed at the values listed in Table 2, while the normalization constants are fitted. *Inset*: The ratio of blackbody normalization constants as a function of rotation phase.

of an additional harder component, especially in the 2004 March spectrum. We do not have enough high-energy information to model this excess quantitatively, but it may represent nonthermal magnetospheric emission similar to the hard X-ray component recently reported from the AXPs 1E 1841–045 (Bassani et al. 2004; Kuiper, Hermsen, & Mendez 2004; Molkov et al. 2004), 1RXS J170849.0–400910 (Revnivstev et al. 2004), and 4U 0142+614 (den Hartog et al. 2004) in *RXTE* and *INTEGRAL* data.

2.2. Pulsed Light Curves and Period Derivative

The quiescent *ROSAT* source was not modulated, with a pulsed fraction upper limit of 24% (Paper I). Since the first detection of pulsed emission in early 2003, the pulsed fraction remained fairly constant at $\approx 54\%$ as seen in the two *Chandra* observations on 2003 August 27 and November 1 (Paper I). The folded light curves from the 2003 September 8 *XMM-Newton* observation (Fig. 4) show that the pulse peak is somewhat narrower than a sinusoid, and the pulsed fractions increase smoothly with energy from 38% at less than 1 keV to $\approx 55\%$ above 5 keV. As discussed in §2.1, the fact that the high-energy light curves do not dip to zero implies that the hot blackbody component is never completely out of view. In 2003 October and 2004 March, the *XMM-Newton* light curves have not changed much. The pulse shape and pulsed fractions are largely unchanged. The marginal appearance of narrow components at the peak of the pulse profile in the highest energy bin may be additional evidence of a hard nonthermal contribution.

The measured barycentric pulse period was 5.539344 ± 0.000019 s on 2003 September 8, and 5.539425 ± 0.000016 s on 2004 March 11 (Table 1), from the combined EPIC pn and MOS data. The measurement from the shorter pn observation of 2003 October 12 has a much larger error bar, but is consistent with the other values. The errors are the 95% confidence level determined from the Z_1^2 test. The two precise period measurements can be compared to yield $\dot{P} = (5.1 \pm 1.6) \times 10^{-12}$ s s $^{-1}$ over the 6 month interval, which implies a characteristic age

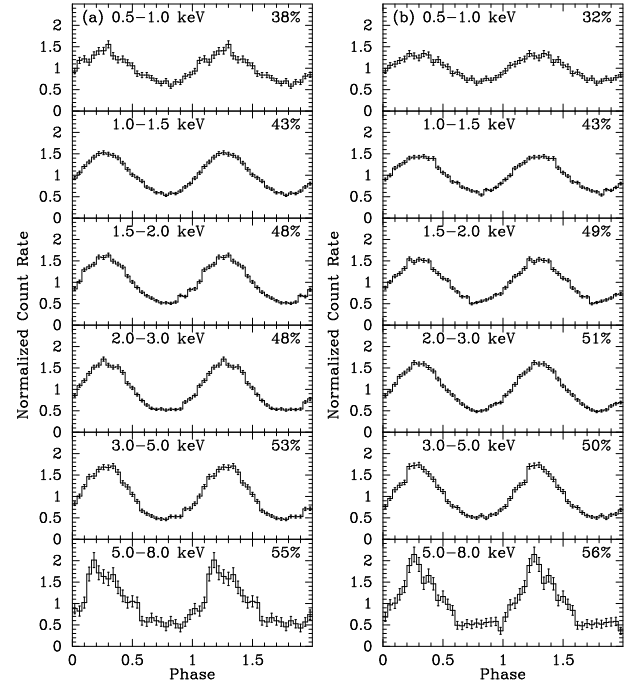


FIG. 4.— Energy-dependent pulse profiles of XTE J1810–197. (a) EPIC pn on 2003 September 8. (b) EPIC pn on 2004 March 11. The epochs of phase zero are given in Table 1. Pulsed fractions, defined as the fraction of the counts above the minimum in the light curve, are indicated in each panel. Background has been subtracted. Pulse profiles from 2003 October 12 (not shown) are similar to these.

$\tau_c \approx 17,000$ yr, surface magnetic field $B_s \approx 1.7 \times 10^{14}$ G, and spin-down power $\dot{E} \approx 1.2 \times 10^{33}$ erg s $^{-1}$, comparable to the earlier values measured by Ibrahim et al. (2004). However, it is evident that \dot{P} is not stable, having varied by at least a factor of 2 on timescales of months. Ibrahim et al. (2004) fitted values of \dot{P} in the range $(1.1 - 2.2) \times 10^{-11}$ s s $^{-1}$ in the first 9 months of the outburst. Increases in \dot{P} of order unity have been seen in the AXPs 1E 2259+586 (Iwasawa, Koyama, & Halpern 1992; Kaspi et al. 2003) and 1RXS J170849.0–400910 (Dall’Osso et al. 2003) following their glitches. Even larger changes in \dot{P} are seen in the SGRs 1900+14 (Kouveliotou et al. 1999; Woods et al. 1999, 2003) and 1806–20 (Woods et al. 2000, 2002), although these were apparently not associated with episodes of bursting. It is possible that XTE J1810–197 experienced a glitch and an increase in \dot{P} at the time of its outburst, and that \dot{P} is now relaxing to its long-term value. Alternatively, the spin-down could have been enhanced in the early stages of the outburst by a particle wind that is now declining. Sufficiently energetic Alfvén waves drive winds that can increase the magnetic field strength at the light cylinder over the dipole value, thereby increasing the spin-down torque. (Thompson & Blaes 1998).

We note here that two discrepant period measurements have been reported from independent analyses of the 2004 March observation. Rea et al. (2004a) gave $P = 5.53974 \pm 0.00005$ s, and later Rea et al. (2004b) gave $P = 5.539917 \pm 0.000005$ s. Both of these are evidently affected by the error in the EPIC pn timing that we discovered in the data (§2). Consequently,

the much larger \dot{P} reported by Rea et al. (2004b) is not valid. Our correct period measurement in Table 1, $P = 5.539425 \pm 0.000016$ s, is confirmed by establishing consistency, both in period and in phase, among the three EPIC instruments' data analyzed separately.

2.3. Long-term Flux Decay

Ibrahim et al. (2004) fitted the decline of the flux from XTE J1810–197 as observed by *RXTE* with either an exponential of time constant 269 ± 25 days, or a power law of $t^{-\beta}$ where $0.45 \leq \beta \leq 0.73$. The allowed range of β comes from the uncertainty in the initial epoch of the outburst, 2003 November 17 < t_0 < 2004 January 23. The new *XMM-Newton* observations extend the baseline by an additional 5.5 months, although it is difficult to make a precise comparison between *RXTE* and *XMM-Newton* fluxes because of the very soft spectrum of the source, and the considerable background and source confusion that plagues *RXTE* in this region of the Galactic plane. Nevertheless, the first *XMM-Newton* observation is consistent in flux with the contemporaneous *RXTE* monitoring (Fig. 1 and Ibrahim et al. 2004), and the September–March *XMM-Newton* points alone fit an exponential time constant of 300 days, marginally consistent with the *RXTE* determined decay. However, if we fit the *XMM-Newton* points with a power-law decay, then the allowed exponent range is $1.03 \leq \beta \leq 1.26$, quite a bit steeper than the *RXTE* fitted rate. Continued monitoring is thus able to discriminate among exponential, power law, or more complicated decays. It already seems that an exponential is a better fit than a power law.

The total energy emitted in the outburst can be estimated by integrating the fitted exponential decay, i.e., multiplying the peak luminosity by the decay constant. Assuming a peak bolometric luminosity of $6 \times 10^{35} d_5^2$ ergs s^{-1} at the onset of the *RXTE* observed outburst (Ibrahim et al. 2004) and a time constant of 300 days yields a fluence of $1.5 \times 10^{43} d_5^2$ ergs.

3. DISCUSSION

3.1. Problems with a Power-Law X-ray Spectrum

A two-component X-ray spectral fit is commonly required for AXPs, but its physical significance is poorly understood. While it is conventional to fit a power-law plus blackbody model, the interpretation of the resulting steep power law, e.g., $\Gamma \approx 3.8$ in the case of XTE J1810–197, is not clear. When employing power laws as a means of fitting excess high-energy emission, problems arising from the dominance of such power laws at low energy are usually ignored. Here, we point out that such a steep power law cannot be connected to the faint IR fluxes measured by Israel et al. (2004) without assuming severe and perhaps unphysical cut-off mechanisms.

According to Figure 5a, which is equivalent to Figure 2 of Israel et al. (2004), the *K*-band measurement and 0.5 keV flux density of XTE J1810–197 as predicted from the power-law fitted component can be bridged by a power law of $F_\nu \propto \nu^\alpha$, where $\alpha = +0.6$. Notably, this value of α is in excess of the low-frequency limit of an optically thin synchrotron spectrum, which has $F_\nu \propto \nu^{+1/3}$. Alternatively, the standard synchrotron self-absorption mechanism, which allows a low-frequency

spectrum $F_\nu \propto \nu^{+5/2}$, can be invoked to avoid exceeding the observed infrared flux. But this would require the self-absorption frequency ν_a to fall in the narrow (and unobservable) range $10^{16} - 10^{17}$ Hz. It also places a requirement on the radius r of the synchrotron source,

$$r = 6 \times 10^{14} B^{1/4} \nu_a^{-5/4} F_{\nu_a}^{1/2} d \text{ cm},$$

where F_{ν_a} is the flux density at ν_a , extrapolated from the fitted X-ray power law. This relation assumes a uniform B field unlike the magnetosphere of a neutron star. But if we combine it with an estimate of the local dipole field at radius r ,

$$B(r) = B_s \left(\frac{r}{12 \text{ km}} \right)^{-3},$$

with $B_s \approx 2 \times 10^{14}$ G, then the synchrotron source must have $r < 3 \times 10^7 d_5^{4/7}$ cm. Such small values of r are inconsistent with the synchrotron assumption since the associated magnetic field $B(r) > 10^{10}$ G is large enough that the soft X-ray spectrum should instead be a broad cyclotron feature. These serious problems with a synchrotron model cast doubt on the utility of a steep power-law fit.

Alternatively, while Thompson, Lyutikov, & Kulkarni (2002) propose that multiple resonant Compton scattering of thermal photons can generate a high-energy tail, this mechanism does not address the origin of the required low-energy excess, which is just as much a part of the steep power-law component as the high-energy tail. Therefore, we conclude that a power law is not a correct description of the actual spectrum. While it fits adequately in the limited X-ray band, it has no compelling physical explanation and is in conflict with lower-energy measurements. Unfortunately, the large column densities to most AXPs prevent an accurate characterization of their intrinsic soft X-ray spectra because the corrections for absorption become highly uncertain when they are large.

The blackbody component in the power-law plus blackbody model is easier to accept since its effective area is initially $\approx 6 \times 10^{11} d_5^2$ cm² (neglecting unknown geometric and beaming factors), decreasing to $\approx 3 \times 10^{11} d_5^2$ cm² in the third observation. Because these areas are both small compared to the surface of the NS, the large pulsed fraction of this component, which dominates the flux from 2–5 keV and does not change as the flux declines, can be understood as rotational modulation of a surface hot spot.

The pulsed light curves provide an independent diagnostic of emission mechanisms. The strict pulse-phase alignment and subtle change of pulse shape as a function of energy in Figure 4 is unnatural under the hypothesis of two entirely different emission mechanisms and locations. The power-law component of the spectral fit dominates below 1.5 keV while the blackbody component dominates between 2 and 6 keV. The observed monotonic increase in pulsed fraction as a function of energy is not accounted for in such a spectral model. This problem applies to AXPs in general, as discussed in detail by Özel, Psaltis, & Kaspi (2001). A hard X-ray tail can arise from radiative transfer effects in a realistically modeled NS atmosphere (Özel 2001; Özel et al. 2001; Perna et al. 2001), thus reducing the need for a power-law component. This

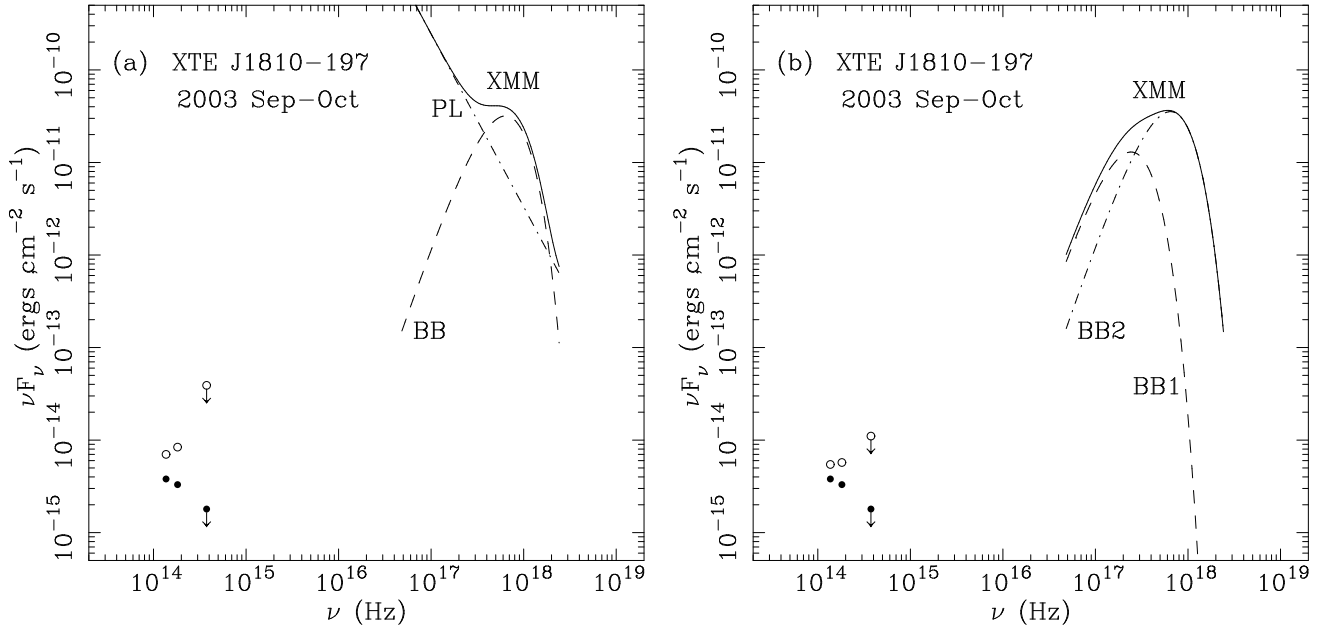


FIG. 5.— Broad-band spectrum of XTE J1810–197 as derived from fits to the *XMM-Newton* EPIC pn data of 2003 September, and contemporaneous infrared and optical data points of Israel et al. (2004) from 2003 October. Filled circles are observed points, and open circles are corrected for extinction using the X-ray fitted N_{H} from each model and the Predehl & Schmitt (1995) relation $N_{\text{H}}/A_{\text{V}} = 1.8 \times 10^{21} \text{ cm}^{-2} \text{ mag}^{-1}$. Fitting parameters of the two-component X-ray spectra are taken from Table 2. The unfolded, unabsorbed spectrum is represented here. (a) Power-law plus blackbody fit to the X-ray spectrum, with $N_{\text{H}} = 1.02 \times 10^{22} \text{ cm}^{-2}$ and $A_{\text{V}} = 5.7 \text{ mag}$. This panel is equivalent to Figure 2 of Israel et al. (2004). (b) Double blackbody fit to the X-ray spectrum, with $N_{\text{H}} = 0.65 \times 10^{22} \text{ cm}^{-2}$ and $A_{\text{V}} = 3.6 \text{ mag}$.

raises the possibility that a purely thermal model may account for the spectra and pulse profiles.

3.2. Advantages of a Purely Thermal X-ray Spectrum

In the alternative double blackbody spectral model, a large area of $\approx 60\%$ the surface of the NS is implied for the cooler blackbody component, while the hotter component has an initial area of $\approx 4\%$ of the NS surface. In its favor, a purely thermal model can explain why the pulsed fraction increases with energy, and why the pulses are in phase at all energies, assuming the geometry to be that of a small hot spot surrounded by a cooler annulus. The phase-resolved spectroscopy discussed in §2.1 supports this picture. Also, the extrapolated X-ray spectrum in this model does not exceed the observed IR fluxes (Fig. 5b). IR and optical emission from AXPs, including XTE J1810–197, are too bright to be surface thermal emission, but are likely to be magnetospheric synchrotron radiation. Unlike the X-rays, the optical/IR emission does not exceed the spin-down luminosity, and could be rotation-powered in quiescence (Özel 2004), although additional energy deposited by magnetic field decay could increase its brightness during outbursts.

Parenthetically, we mention the case of the AXP 1RXS J170849.0–400910. A double blackbody was also one of the models fitted to the X-ray spectrum of 1RXS J170849.0–400910 by Israel et al. (2001), with an interpretation similar to ours. On the other hand, 1RXS J170849.0–400910 is unique among AXPs for having a strong energy dependence of its pulse phase, shifting by ≈ 0.3 cycles between 2 and 10 keV. Rea et al. (2003) interpret this as most likely due to a phase dependence of a power-law spectral index. Interestingly, this is the

only AXP for which good evidence of a cyclotron absorption feature is found, at 8.1 keV (Rea et al. 2003), and therefore a true deviation from blackbody emission.

While a purely thermal model may be favored by the simple arguments presented above, detailed modeling of the light curves will be needed to verify that the softest X-rays from XTE J1810–197, which come from the cooler, larger area blackbody, can have a pulsed fraction as high as the observed 38%. The emitting area might be even larger if realistic atmosphere models are fitted instead of pure blackbodies (Perna et al. 2001). One possibility is that d is considerably less than 5 kpc, thus reducing the emitting area. Another important consideration is the effect of realistic radiative transfer in highly magnetized atmospheres. Özel et al. (2001) showed that the sorts of pulsed light curves that are observed from XTE J1810–197 and other AXPs are inconsistent with two antipodal hot spots on the surface. However, they showed that a single hot spot is capable of producing large pulsed fractions as well as the observed energy dependence from a nearly orthogonal rotator if the magnetic field is assumed to be normal to the surface. [Note that Özel et al. (2001) use a different definition of pulsed fraction from the one that we use in Figure 4]. The large predicted pulsed fractions rely on the “beaming” effect of anisotropic radiative transfer in a large magnetic field, in which the electron scattering cross sections of both the ordinary and extraordinary modes of polarization are minimized where the angle between the wave vector \mathbf{k} and the magnetic field \mathbf{B} is zero.

The quiescent *ROSAT* spectrum of XTE J1810–197 is fitted by a simple blackbody comparable to the full

surface area of a NS. Note that the temperature measured by *ROSAT* using a single blackbody model is even lower than found for the cooler component of the two-temperature *XMM-Newton* fit. This perhaps accounts for the failure to detect rotational modulation in the quiescent state. Thus, it is possible that the X-ray manifestation of the outburst of a TAXP is largely due to a sudden thermal heating event in the crust, while the long-term quiescent flux is powered by slow dissipation of the core magnetic field (Thompson & Duncan 1996) or simply by residual cooling in the presence of an insulating atmosphere of hydrogen or helium (Heyl & Hernquist 1997).

3.3. Afterglow Following Deep Crustal Heating

Similar to XTE J1810–197, a decay of the thermal component in the AXP 1E 2259+586 was seen during the bursting episode in 2002 June (Woods et al. 2004), when a small, hot region of $kT_{\text{BB}} \approx 1.7$ keV and $R \approx 1$ km cooled within one day, leaving a quiescent thermal component of $kT_{\text{BB}} \approx 0.5$ keV and $R \approx 6$ km. After 1 day, the 2–10 keV X-ray flux decayed further as a slow $t^{-0.22}$ power law for at least 200 days. Hot spots due to deep crustal heating by localized magnetic field decay, or surface bombardment by accelerated particles, can plausibly produce the observed spectra and pulse profiles. However, heating by magnetic field decay is preferred over particles accelerated only on open field lines in the dipole geometry, since the canonical dipole polar cap area is only $2 \times 10^8 (P/5.5 \text{ s})^{-1} \text{ cm}^2$ for such slow rotators as these AXPs, much smaller than the detected areas.

Eichler et al. (2003) reviewed mechanisms for “afterglows” from cooling of the crust following SGR like outbursts in magnetars. Deep crustal heating that is subject to a long conduction time to the surface can plausibly be the cause. Thompson et al. (2002) showed that the resulting cooling would follow a $t^{-0.7}$ power law. The initial heating could take place within 10^4 s due to large-scale shearing of the crust by magnetic stresses. Lyubarsky, Eichler, & Thompson (2002) assumed a deposition of $\sim 10^{25}$ ergs cm^{-3} to a depth of 500 m, which is $\leq 1\%$ of the magnetic energy density at the surface. If occurring over the entire surface, this is $\sim 1 \times 10^{43}$ ergs, comparable to the total X-ray energy emitted during the decay of XTE J1810–197. If such releases occur with recurrence time > 20 yr, AXPs could power transient outbursts for > 5000 yr. However, this simple rate estimate does not take into account heat conduction into the core of the NS. Lyubarsky et al. (2002) find that only 20% of the deposited heat is radiated during the afterglow; the rest is conducted into the interior and contributes to the average quiescent X-ray or neutrino emission. The observed quiescent luminosity of 1.3×10^{34} ergs s^{-1} could be powered by $\sim 7 \times 10^{45}$ ergs of magnetic energy dissipated in the core over the presumed $\sim 17,000$ yr age of the NS.

This theory has been applied to the slow cooling observed from SGR 1900+14 (Ibrahim et al. 2001; Woods et al. 2001; Lenters et al. 2003) and SGR 1627–41 (Kouveliotou et al. 2003; Lyubarsky et al. 2002) following their outbursts. In the spectra of SGR 1900+14, a blackbody component was identified that has a high initial temperature, ≈ 2 keV, and radius of ≈ 1.7 km, much smaller than a neutron star, showing that heating

(or heat conduction or radiation) can indeed be localized. Therefore, it seems that the long timescale decay of the flux from XTE J1810–197 could be due to the same process that occurs in the outbursts of SGRs.

While there are still too few measurements to characterize reliably the long-term decay of the outburst of XTE J1810–197, it does seem already to be declining faster than the $t^{-0.7}$ power law predicted in the crustal heating model. We find a decay index of 1.03–1.26 in the interval 9–15 months after the presumed outburst, but an exponential of time constant 300 days is a better description of the entire light curve since outburst. Similar deviations of the post-outburst decay curve of SGR 1627–41 from a power law (Kouveliotou et al. 2003) complicate the crustal heating interpretation. Of course, the existing cooling models are based on solving a one-dimensional heat transfer equation, and do not involve localized heating and possible changes in emitting area such as are suggested by the observations of XTE J1810–197.

Another variable AXP for which detailed spectral analysis at different intensity levels has been performed is 1E 1048.1–5937. Mereghetti et al. (2004) found that its spectral shape remained invariant between states of luminosity that differed by a factor of 5. In a fitted two-component model, the power-law index as well as the blackbody temperature remained the same, which implies that it is not realistic to assume two physically distinct emission mechanisms. Instead, the variability in flux could be explained in a purely thermal model by a change in emitting area. Such an interpretation would be consistent with the pulsed fraction of the light curve of 1E 1048.1–5937, which decreased as the flux increased (Mereghetti et al. 2004). We interpret the decay of XTE J1810–197 along the same lines.

4. CONCLUSIONS AND FUTURE WORK

We used three *XMM-Newton* observations of XTE J1810–197 obtained during its decline from outburst to make a number of quantitative measurements, although their robustness needs to be tested with additional follow-up observations. The decay is consistent with an exponential of time constant ≈ 300 days. The pulsar spin-down rate is quite variable, having decreased to $(5.1 \pm 1.6) \times 10^{-12} \text{ s s}^{-1}$ after initial measurements by *RXTE* found it to vary in the range $(1 - 2) \times 10^{-11} \text{ s s}^{-1}$. The inferred characteristic age $\tau_c \approx 17,000$ yr, magnetic field strength $B_s \approx 1.7 \times 10^{14}$ G, X-ray spectra, and pulsed light curves, are all consistent with the behavior of an anomalous X-ray pulsar, albeit one that has varied in flux by two orders of magnitude. Assuming that the decay continues at the observed exponential rate, the total energy radiated in the present outburst will be $\approx 1.5 \times 10^{43} d_5^2$ ergs. This is comparable to the heat that can be deposited in the crust by conversion of $< 1\%$ of the magnetic energy density at the surface. Such a magnetar mechanism could power outbursts similar to the current one at > 20 yr intervals for a large fraction of the characteristic age of the pulsar, while the quiescent luminosity observed in a number of archival X-ray observations could come from the long-term average magnetic decay heating of the NS core. Models of deep crustal heating typically predict $t^{-0.7}$ power-law decays, which are not matched by the sparse measurements

so far obtained from XTE J1810–197. However, more complex decay behavior has been seen in several other magnetars, which may require refinements to the initial simple models, in particular, generalization to two dimensions.

The X-ray spectrum and pulse profiles of XTE J1810–197 are typical of AXPs. We discussed the problems with allowing a power-law plus blackbody fit, which results in a steep power law that is difficult to reconcile with the faintness of the optical/IR counterpart. The lack of variation in pulse profile as a function of energy also argues against the action of two different emission mechanisms. Instead, a purely thermal model for the spectrum, here adequately modeled as two temperatures, is more physically motivated. The required blackbody areas are less than or equal to the surface area of a neutron star, and the pulse modulation can probably be understood in terms of anisotropic heat conduction and radiative transfer in the strong magnetic field. Two dimensional cooling models will be required to explain why the decay is characterized as a decline in emitting area rather than temperature, the latter remaining constant, at least initially. The spectral data obtained so far are limited in that the existing *XMM-Newton* observations span slightly less than a factor of 2 in luminosity. The most stringent constraints on models may yet come from X-ray spectra and pulse profiles to be obtained over the coming years, as the luminosity of XTE J1810–197 is still a factor of 20–30 above its historic quiescent level.

The existence of serendipitous archival data allowed us to determine that XTE J1810–197 lacked pulsations in the quiescent state preceding the current outburst. This suggests that CCOs may be interpreted as quiescent AXPs. No periodic signals have been detected so far from the CCOs in the Cas A, Puppis A, and Kes 79 SNRs, for example. Cas A is known to be a very young, ≈ 300 yr object; its central source has a spectrum consistent with an AXP (Chakrabarty et al. 2001; Mereghetti, Tiengo, & Israel 2002). A similar object may be the point source at the center of Kes 79 (Seward et al. 2003). The radio quiet neutron star RX J0822–4300 in Puppis A also has a spectrum sim-

ilar to that of XTE J1810–197 (Becker & Aschenbach 2002). Gaensler, Bock, & Stappers (2000) argue that RX J0822–4300 may have AXP-like spin parameters. The CCO in SNR RCW 103, a non-pulsating AXP-like object, has been monitored for over a decade and it is found to display marked variability on months to hours time scales. [While a possible 6 hr periodic variation suggests that this object is a low-mass binary (Becker & Aschenbach 2002; Sanwal et al. 2002), the evidence is not conclusive.] SGRs are hypothesized to be older ($\sim 10^4$ yr) manifestations of the AXPs (Gotthelf, Vasisht, & Dotani 1999b; Gaensler et al. 2001). AXPs and SGRs have long been considered related phenomena, reinforced by the recent detection of SGR-like bursts from the two AXPs 1E 1048.1–5937 and 1E 2259+586 (Gavriil, Kaspi, & Woods 2002; Kaspi et al. 2003). The various “classes” of young NSs that differ significantly from rotation-powered pulsars are phenomenologically related, possibly through an evolutionary progression.

Although TAXPs are relatively rare, their short active duty cycle suggests the existence of a larger population of unrecognized young NSs. To this end, XTE J1810–197 provides a unique window into this population, with prior measurements in the quiescent state and detailed observations during its active, pulsed phase. It is important to monitor closely the fading of XTE J1810–197 during this possibly one-time opportunity to study the processes of thermal and non-thermal emission to which magnetars convert their energy. Measurement of the quiescent spectrum is especially important to help identify the faint population of likely missed NSs.

This investigation is based on observations obtained with *XMM-Newton*, an ESA science mission with instruments and contributions directly funded by ESA Member States and NASA. We thank R. Warwick and D. J. Helfand for providing the 2003 October data from the *XMM-Newton* Galactic Plane Survey. This work was also supported by NASA *RXTE* grant NNG04GF59G to J.P.H., and NASA LTSA grant NAG 5-8063 to E.V.G.

REFERENCES

- Anders, E., & Ebihara, M. 1982, *Geochim. Cosmochim. Acta*, 46, 2363
- Bassani, L., et al. 2004, *Astronomer’s Telegram*, 232
- Becker, W., & Aschenbach, B. 2002, in *Proc. 270 WE-Heraeus Seminar, Neutron Stars, Pulsars, and Supernova Remnants*, ed. W. Becker, H. Lesch, & J. Trümper, MPE Report 278, p. 64
- Chakrabarty, D., Pivovarov, M. J., Hernquist, L. E., Heyl, J. S., & Narayan, R. 2001, *ApJ*, 548, 800
- Dall’Osso, S., Israel, G. L., Stella, L., Possenti, A., & Perozzi, E. 2003, *ApJ*, 599, 485
- den Hartog, P. R., Kuiper, L., Hermsen, W., & Vink, J. 2004, *Astronomer’s Telegram*, 293
- Duncan, R. C., & Thompson, C. 1992, *ApJ*, 392, L9
- Eichler, D., Lyubarsky, Y., Thompson, C., & Woods, P. 2003, in *Pulsars, AXPs, and SGRs Observed with BeppoSAX and Other Observatories* (astro-ph/0303296)
- Gaensler, B. M., Bock, D. C.-J., & Stappers, B. W. 2000, *ApJ*, 537, L35
- Gaensler, B. M., Slane, P. O., Gotthelf, E. V., & Vasisht, G. 2001, *ApJ*, 559, 963
- Gavriil, F. P., & Kaspi, V. M., & Woods, P. M. 2002, *Nature*, 419, 142
- Gotthelf, E. V., Halpern, J. P., Buxton, M., & Bailyn, C. 2004, *ApJ*, 605, 368 (Paper I)
- Gotthelf, E. V., Petre, R., & Hwang, U. 1997, *ApJ*, 487, L175
- Gotthelf, E. V., Petre, R., & Vasisht, G. 1999a, *ApJ*, 514, L107
- Gotthelf, E. V., & Vasisht, G. 1998, *NA*, 3, 293
- Gotthelf, E. V., Vasisht, G., & Dotani, T. 1999b, *ApJ*, 522, L49
- Green, D. A., Gull, S. F., Tan, S. M., & Simon, A. J. B. 1988, *MNRAS*, 231, 735
- Hands, A. D. P., Warwick, R. S., Watson, M. G., & Helfand, D. J. 2004, *MNRAS*, 351, 31
- Heyl, J. S., & Hernquist, L. 1997, *ApJ*, 489, L67
- Ibrahim, I. A., et al. 2001, *ApJ*, 558, 237
- Ibrahim, I. A., et al. 2004, *ApJ*, 609, L21
- Israel, G. L., Oosterbroek, T., Stella, L., Campana, S., Mereghetti, S., & Parmar, A. N. 2001, *ApJ*, 560, L65
- Israel, G. L., et al. 2004, *ApJ*, 603, L97
- Iwasawa, K., Koyama, K., & Halpern, J. 1992, *PASJ*, 44, 9
- Kaspi, V. M., Gavriil, F. P., Woods, P. M., Jensen, J. B., Roberts, M. S. E., & Chakrabarty, D. 2003, *ApJ*, 588, L93
- Kouveliotou, C., et al. 1999, *ApJ*, 510, L115
- Kouveliotou, C., et al. 2003, *ApJ*, 596, L79
- Kuiper, L., Hermsen, W., & Mendez, M. 2004, *ApJ*, submitted (astro-ph/0404582)
- Lenters, G. T., Woods, P. M., Goupell, J. E., Kouveliotou, C., Göögüs, E., Hurley, K., Frederiks, D., Golenetskii, S., & Swank, J. 2003, *ApJ*, 587, 761
- Lyubarsky, Y., Eichler, D., & Thompson, C. 2002, *ApJ*, 580, L69
- Marsden, D., & White, N. E. 2001, *ApJ*, 551, L155
- Mereghetti, S., Tiengo, A., & Israel, G. L. 2002, *ApJ*, 569, 275

- Mereghetti, S., Tiengo, A., Stella, L., Israel, G. L., Rea, N., Zane, T., & Oosterbroek, T. 2004, *ApJ*, 608, 427
- Molkov, S. V., Cherepashchuk, A. M., Lutovinov, A. A., Revnivstev, M. G., Postnov, K. A., & Sunyaev, R. A. 2004, *Astronomy Letters*, in press (astro-ph/0402416)
- Morrison, R., & McCammon, D. 1983, *ApJ*, 270, 119
- Özel, F. 2001, *ApJ*, 563, 276
- Özel, F. 2004, *ApJ*, submitted (astro-ph/0404144)
- Özel, F., Psaltis, D., & Kaspi, V. M. 2001, *ApJ*, 563, 255
- Perna, R., Heyl, J. S., Hernquist, L. E., Juett, A. M., & Chakrabarty, D. 2001, *ApJ*, 557, 18
- Predehl, P., & Schmitt, J. H. M. M. 1995, *A&A*, 293, 889
- Rea, N., Israel, G. L., Stella, L., Oosterbroek, T., Mereghetti, S., Angelini, L., Campana, S., & Covino, S. 2003, *ApJ*, 586, L65
- Rea, N., et al. 2004a, *Astronomer's Telegram* 284
- Rea, N., et al. 2004b, *A&A*, 425, L5
- Revnivstev, M. G., et al. 2004, *Astronomy Letters*, 30, 382
- Sanwal, D., Garmire, G. P., Garmire, A., Pavlov, G. G., & Mignani, R. 2002, *BAAS*, 34, 764
- Seward, F. D., Slane, P. O., Smith, R. K., & Sun, M. 2003, *ApJ*, 584, 414
- Thompson, C., & Blaes, O. 1998, *Phys. Rev. D*, 57(6), 3219
- Thompson, C., & Duncan, R. C. 1996, *ApJ*, 473, 322
- Thompson, C., Lyutikov, M., & Kulkarni, S. R. 2002, *ApJ*, 574, 332
- Turner, M. J. L., Briel, U. G., Ferrando, P., Griffiths, R. G., & Villa, G. E. 2003, *SPIE*, 4851, 169
- Vasisht, G., Aoki, T., Dotani, T., Kulkarni, S. R., & Nagase, F. 1996, *ApJ*, 456, L59
- Woods, P. M., Kaspi, V. M., Thompson, C., Gavriil, F. P., Marshall, H. L., Chakrabarty, D., Flanagan, K., Heyl, J., & Hernquist, L. 2004, *ApJ*, 605, 378
- Woods, P. M., Kouveliotou, C., Göğüş, E., Finger, M. H., Swank, J., Markwardt, C. B., Hurley, K. H., & van der Klis, M. 2002, in *ASP Conf. Ser. 271, Neutron Stars in Supernova Remnants*, ed. P. O. Slane & B. M. Gaensler (San Francisco: ASP), 313
- Woods, P. M., Kouveliotou, C., Göğüş, E., Finger, M. H., Swank, J., Smith, D. A., Hurley, K., & Thompson, C. 2001, *ApJ*, 552, 748
- Woods, P. M., et al. 1999, *ApJ*, 524, L55
- Woods, P. M., et al. 2000, *ApJ*, 535, L55
- Woods, P. M., et al. 2003, *ApJ*, 596, 464